Appl. Phys. B (2017) 123:204
DOI 10.1007/s00340-017-6762-3

Applied Physics B
Lasers and Optics

Energetic metallic ion implantation in polymers via cost-effective laser-driven ion source

Muhammad Bilal Tahir[1] · M. Shahid Rafique[2] · Rabia Ahmed[2] · M. Rafique[1] · Tahir Iqbal[1] · Ali Hasan[1]

Received: 17 February 2017 / Accepted: 29 May 2017 / Published online: 28 June 2017

Abstract This research work reports the ions emission from the plasma generated by Nd:YAG laser having wavelength 1.064 μm, power 1.1 MW, pulse energy 10 mJ and intensity 10^{11} W/cm^2 irradiated at 70° with respect to the target normal to the ions. These ions were accelerated through a home-made extraction assembly by means of a high voltage DC power supply. The energy of these ions were measured using Thomson parabola technique which utilizes Solid State Nuclear Track Detector (CR-39) and confirmed by Faraday cup as well that exploits a well-known technique known as time of flight. Interestingly, a significant increase in energy (from 490 to 730 keV) was observed with a discrete increase in acceleration potential from 0 to 18 kV. Polyethylene terephthalate (PET) and polypropylene were exposed to this recently developed ion source facility, to authenticate the reliability of this facility. The surface of the polymer is affected when energy of the irradiated ion is increased, which is evident from the optical micrographs. An increase in electrical conductivity was also observed with the increase in ion energy.

1 Introduction

Ion implantation process is a powerful tool for the surface modification of materials by introducing a controlled amount of highly energetic ions into a skin layer. Surface etching and ion implantation processes have been benefited drastically by the improvement of laser ion source (LIS) [1–7]. The technique of ion implantation is executed in two ways, i.e., direct ion implantation and through acceleration of ions by applying an external voltage. Direct ion implantation needs a high power laser system, whereas ion implantation through laser-induced plasma driven by an external electric field seems to be a more accessible, efficient and flexible skill [7, 8]. The issue of energetic ions–matter interaction remains a challenge for physicists over the past decades because of its applications in basic and applied field, i.e., industry. Recently, there is intense interest in studying ion beam modifications of polymeric materials. Interactions between energetic ions and the material take place at the cost of the initial kinetic energy of the ion [9–12]. The laser-generated plasma ion implantation-induced polymer amendment is found to produce a spectrum of new properties, e.g., significant changes in conductance, optical and magnetic characteristics, surface hardness, adhesion and other parameters, reviewed in relation to sensible applications [13–17]. The effect of highly energetic ion implantation (as a type of environmentally friendly physical surface modification technology) on structure and composition of polymers is intricate [18, 19]. Various physical and chemical phenomena can result through the interaction of the impacting ions with the polymeric material. These processes strongly depend on the energy of the implanted ion and the mechanisms of energy transfer which may lead to structural and compositional changes in the polymer [20–22].

Metal ion-implanted polymers with enhanced electrical conductivity are commercially important in applications where dispensation of large area components at low material cost is essential, but they are not likely to compete in areas where large mobilities are mandatory.

✉ Muhammad Bilal Tahir
m.bilaltahir@uog.edu.pk

[1] Department of Physics, Faculty of Sciences, University of Gujrat, Hafiz Hayat Campus, Gujrat 50700, Pakistan

[2] Department of Physics, University of Engineering and Technology (UET), Lahore, Pakistan

In this way, the ion-implanted polymers may fill up the fissure (gap) [23–25]. The fabrication of planar resistors is a promising application of polymers with a conductive surface layer created by means of ion implantation. The benefit of the ion implantation technique is the possibility to control the electrical resistivity in a very wide range from 10^{-2} to 10^{16} Ω cm by changing the energy and dose of ion and the type of polymer. As the change in the electrical resistivity is intimately linked to deep structural compositional changes of the polymer, the resulting structure of the resistor is expected to demonstrate high stability [26–30]. Implantation of energetic ions can create a buried conductive layer in the polymer, i.e., a sandwiched structure of the type: porous low-conducting surface layer/buried conductive layer/insulating bulk material is fashioned [31–34]. This type of structure makes it possible to organize the transconductance of the buried layer as a result of ion implantation, by applying an external electric field. This technology seems to open a way for fabrication of field effect transistor-like electronic switches [35–37]. The control of polymer conductance by high-energy ion irradiation is of enormous significance, as implanted polymeric materials can be used as active elements of electronic devices [13, 38]. A drawback of the radiation-modified polymers is the low mobility of charge carriers. However, fair prices and specific properties such as plasticity as well as stable reliance of the conductance on temperature provide them an advantage to be employed for fabrication of resistors and temperature sensors [39–42].

The fabrication of home-made tabletop and cost-effective laser-driven ion accelerator as ion source has been recently motivated by the applications of ion beams for surface modifications of different materials, depositing thin films, construction of hybrid ion sources and many other applications. Additionally, among the advantages of employing laser ion source are: the ability to ionize each and every element, from non-conductive to refractory material; high ion yield per laser shot; easy operation; the easiness to produce plasma utilizing commercially available lasers of high power; production of high charge state ions; high implantation rate; the possibility to get mixed ion beams by irradiation of multi-elemental targets; and low operational cost.

In the current experimental work, Nd:YAG laser (1064 nm, 9–14 ns, and 10 mJ) was used to irradiate the copper target (Cu) for the production of laser-generated ions. Laser-driven ion accelerator was used to enhance the energy of the laser-generated Cu ions. For this purpose, an external high voltage (up to +18 kV) was applied to the extraction box as well as to the target material. The kinetic energy was calculated by means of the Thomson parabola technique and time of flight method using two Faraday cups as well. After the calculation of average kinetic energy of Cu ions, various polymers such as PET and polypropylene with thickness of 73 and 350 μm, respectively, were irradiated by these ions to investigate the surface morphological changes and modification of electrical properties.

2 Experimental setup

The Nd:YAG laser of 1064 nm wavelength, with 10 mJ energy pulse, 1.1 MW power, pulse duration 9–14 ns with a resulting intensity of 10^{11} W/cm^2, was focused onto the solid target using infrared (IR) lens (f = 19 cm) at 70° angle of incidence with respect to the target normal, to produce laser-generated ions. An ion extraction chamber was required to avoid arcs. It is an almost hermetic rectangular box, 24 cm long, 19.5 cm width and 19.5 cm height, having a laser entrance port and a port (3.8 length) along the longitudinal direction of the chamber necessary for ion extraction.

The Nd:YAG laser beam entered the stainless steel chamber through a thin IR window with germanium coating and was focused through the lens to irradiate the metallic target. Directed laser energy impact on matter leads to heating and consequent plasma formation. In general, the electron-lattice relaxation time, in metals, is 1–10 ps. Thermal ablation occurs when the laser pulse width is longer than the electron–lattice relaxation time. For nanosecond laser–matter interaction, the process of laser–target interaction is thermodynamic and the plasma is produced by evaporation of the heated material. Following the generation of plasma, the rest of the laser pulse is used to heat the plasma, instead of contacting the target material. Emission of ions from the laser-induced plasma takes place due to a self-generated electric field. The energy of the emitted ions is low and was enhanced while providing accelerating voltage in the chamber. Therefore, an extraction chamber was designed with grounded electrode to accelerate the laser-generated ions. High positive voltage up to 18 kV was provided to the target that was mechanically and electrically connected to the extraction chamber. The potential of the acceleration system was controlled by positive high-voltage DC power supply and varied from 0 to +18 kV with a stepwise voltage of 2 kV and a current of 3 mA. A grounded electrode in front of an extraction chamber, fixed 2.5 cm away, allowed generating an intense electric field, which was able to extract and accelerate the Cu ions. Both extraction chamber and vacuum chamber were grounded to avoid sparks at such a high DC voltage. A scheme of the ion beam measurement by Faraday cups using the time of flight method is shown in Fig. 1 [39]. Two Faraday cups were placed in the port of the stainless steel chamber, at a distance of 2 cm from the grounded electrode

to the first cup, to determine the average kinetic energy of the extracted Cu ions by the time of flight method. After the in situ measurement, the Faraday cups were replaced by a substrate holder as shown in Fig. 2 [39]. The separation between the grounded electrode and the substrate was 2 cm. The technique of acceleration and the geometry of the experimental configuration were properly planned and employed to avoid arcing in the plasma and, in some case, the deposition of the neutral component on the surface of the substrate.

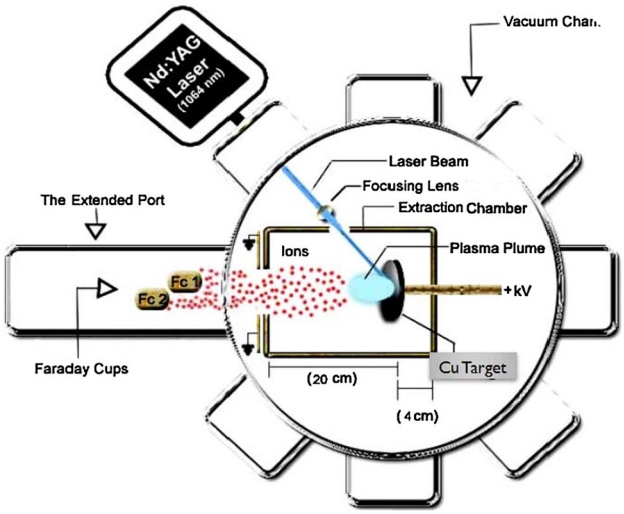

Fig. 1 Schematic diagram to measure the average kinetic energy of Cu ions by the time of flight method

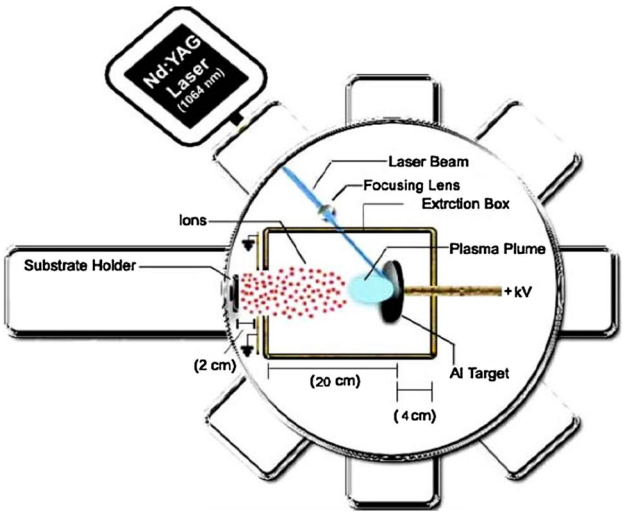

Fig. 2 A scheme showing irradiation of the polymeric medium by energetic ions

3 Results and discussions

The signal profiles of the accelerated ions were stored by a four-channel 500 MHz digital storage oscilloscope. The electrical properties of polyethylene terephthalate (PET) and polypropylene caused by the impinging ions were investigated by a four-point probe, while the modified surface properties of the polymers were investigated using an optical microscope.

3.1 Signal profiles of Cu ions and morphologies of implanted polymers

Figure 3 shows that plot of acceleration voltage versus the kinetic energy of the laser-generated ions. It was found that the kinetic energy of the accelerated ions increases by increasing the applied external voltage. Figure 4 shows the optical micrographs of the pristine sample of PET and polypropylene taken at 200× magnification. It was observed that there was no destruction or any affected part at the surface of both the substrates, but there were some scratches and the skin layer of the sample was not entirely smooth.

Figures 5a, 6a, 7a, 8a, 9a, 10a, 11a, 12a, 13a and 14a show the signal profiles of laser-generated Cu ions stored by the digital oscilloscope with the help of a Faraday cup (time of flight method) that was used to verify the energy of the accelerated ions, which was measured by the Thomson parabolic technique as well. The average kinetic energy of Cu ions was calculated (Table 1). The Nd:YAG laser beam of intensity 10^{11} W/cm^2 was sufficient to generate singly and doubly charged states of metallic Cu ions. At channel 1, various bursts of singly

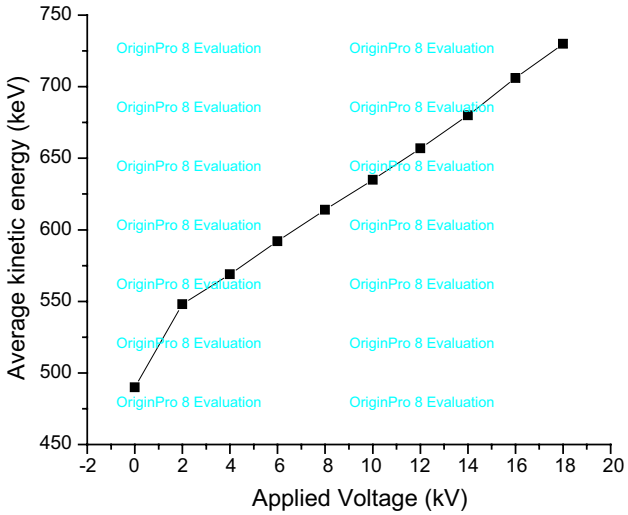

Fig. 3 Acceleration voltage across the average kinetic energy of Cu ions

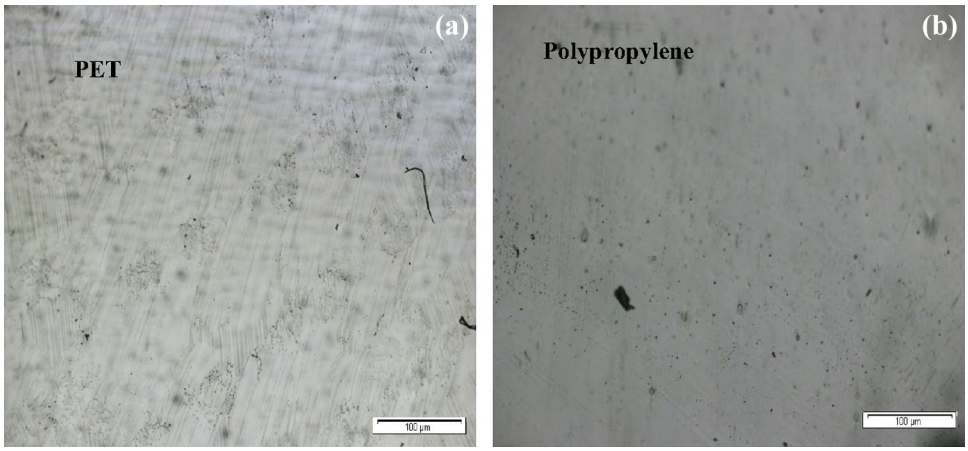

Fig. 4 Optical micrographs of pristine, **a** PET, **b** polypropylene (×200 magnification)

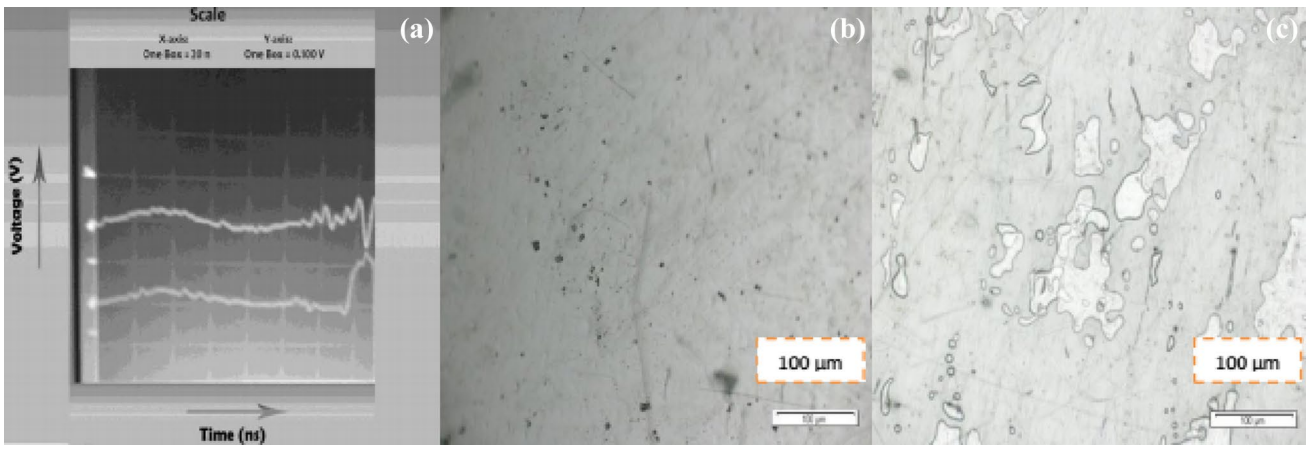

Fig. 5 **a** Faraday cup signal profile of 490 keV Cu ions without acceleration voltage and optical micrographs of 490 keV ion irradiated, **b** PET and **c** polypropylene (×200 magnification)

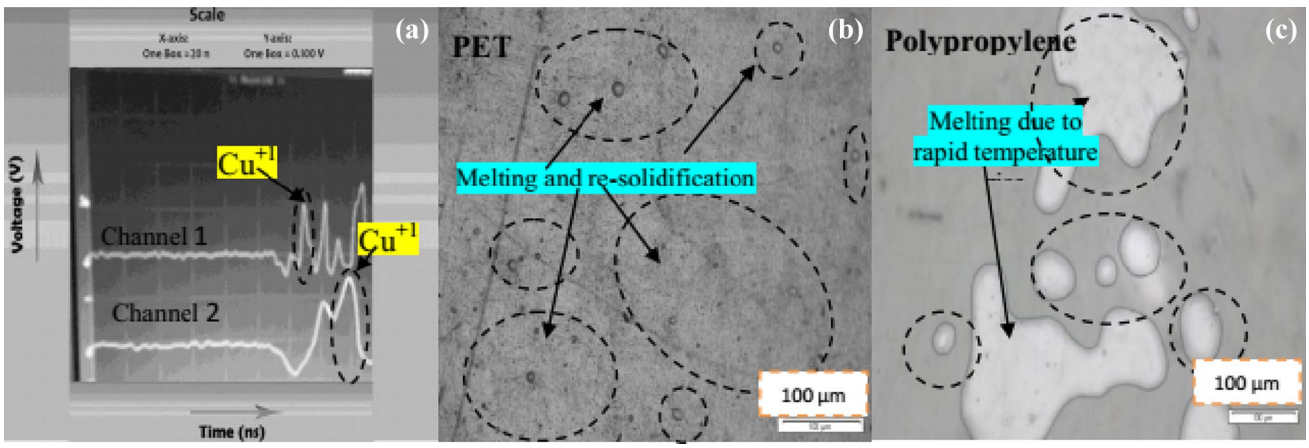

Fig. 6 **a** Faraday cup signal profile of Cu ions at an acceleration voltage of 2 kV and optical micrograph ion irradiated, **b** PET, and **c** polypropylene (×200 magnification)

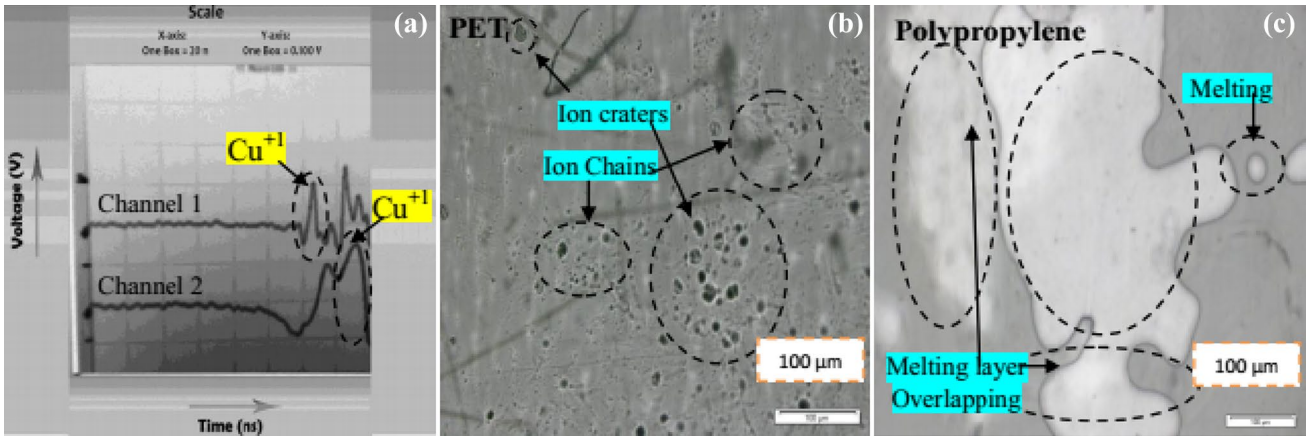

Fig. 7 **a** Faraday cup signal profile of Cu ions in air at an acceleration voltage of 4 kV and optical micrographs of ion irradiated, **b** PET, and **c** polypropylene (×200 magnification)

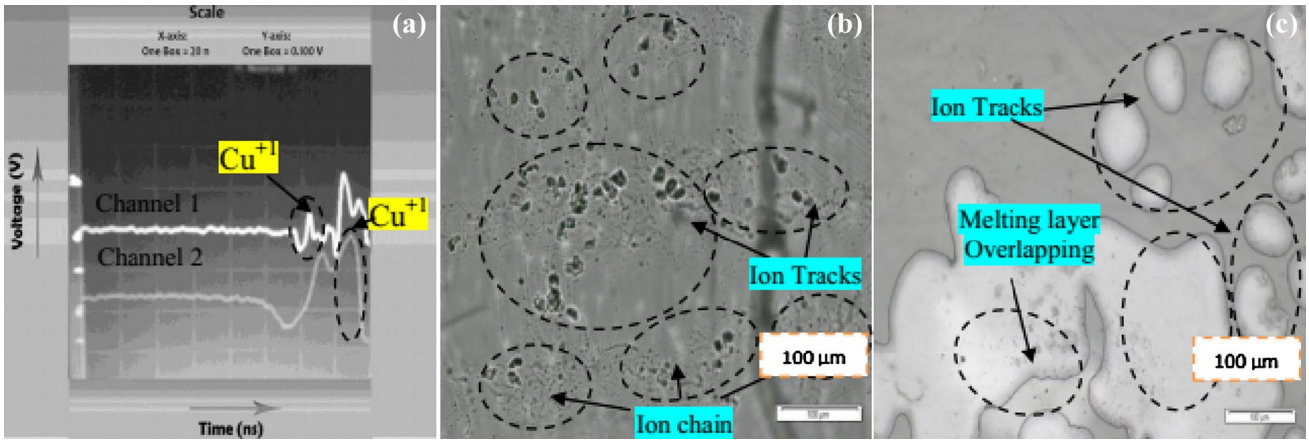

Fig. 8 **a** Faraday cup signal profile of Cu ions in air at an acceleration voltage of 6 kV and optical micrographs of ion irradiated, **b** PET, and **c** polypropylene (×200 magnification)

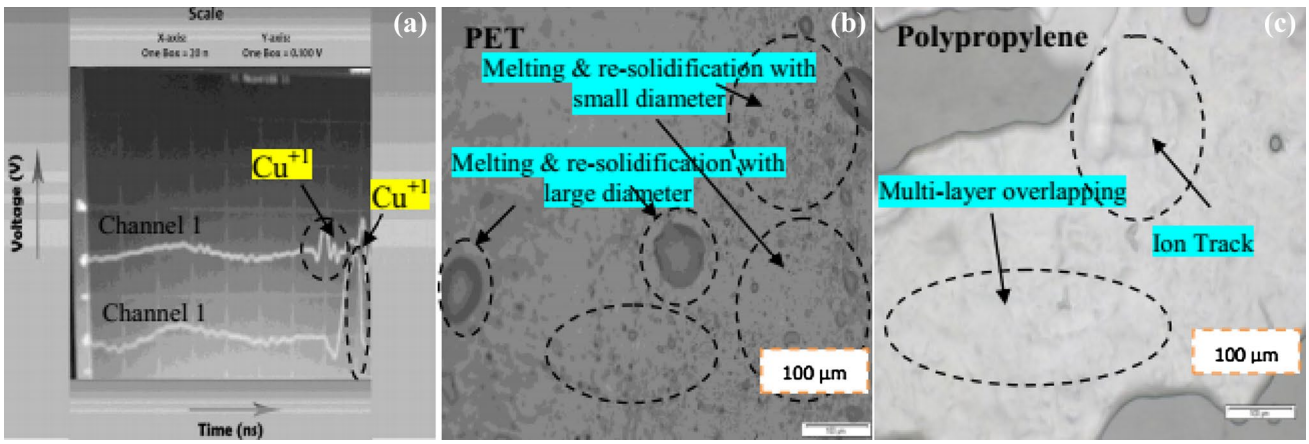

Fig. 9 **a** Faraday cup signal profile of Cu ions in air at an acceleration voltage of 8 kV and optical micrographs of ion irradiated, **b** PET and **c** polypropylene (×200 magnification)

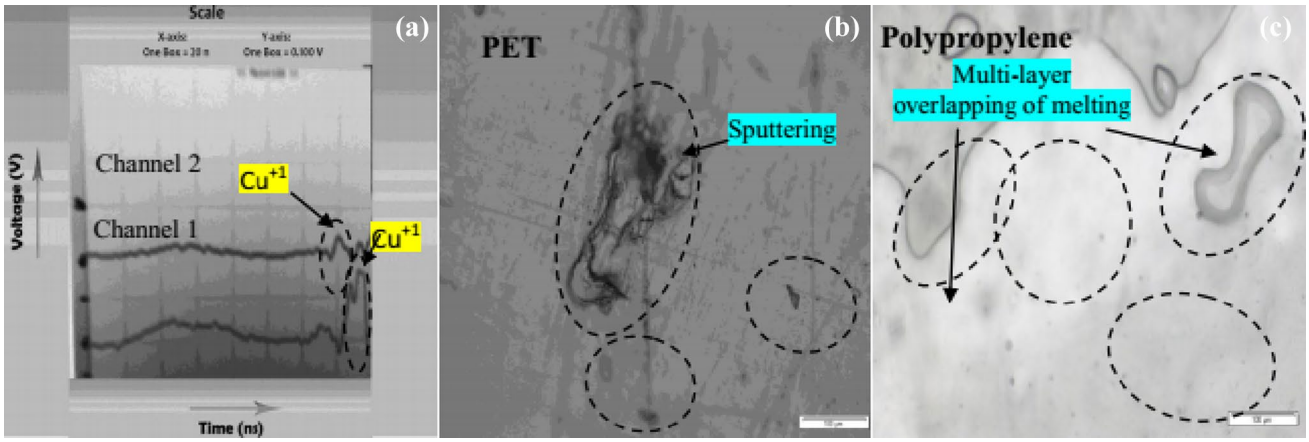

Fig. 10 **a** Faraday cup signal profile of Cu ions in air at an acceleration voltage of 10 kV and optical micrographs of ion irradiated, **b** PET, and **c** polypropylene (×200 magnification)

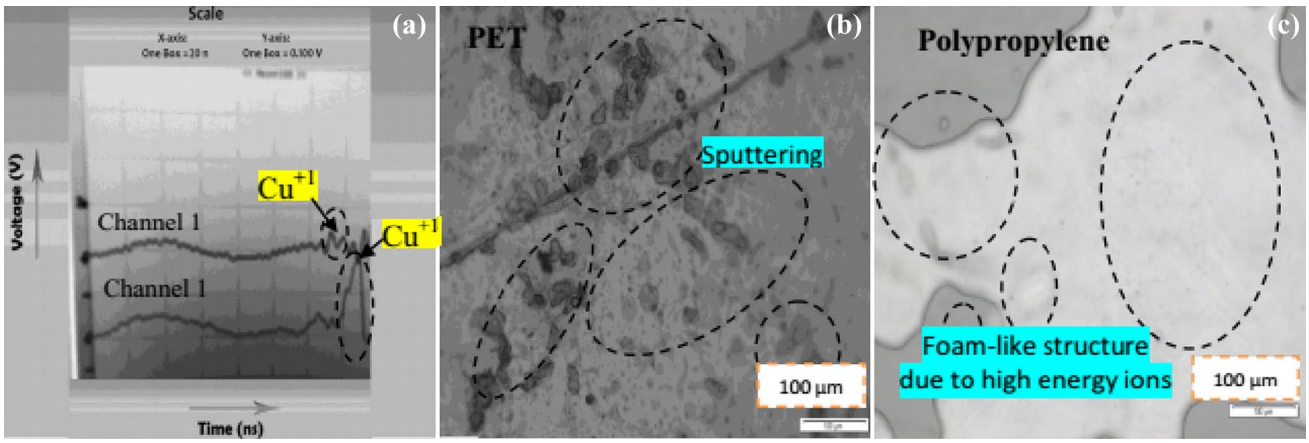

Fig. 11 **a** Faraday cup signal profile of Cu ions in air at an acceleration voltage of 12 kV and optical micrographs of ion irradiated, **b** PET, and **c** polypropylene (×200 magnification)

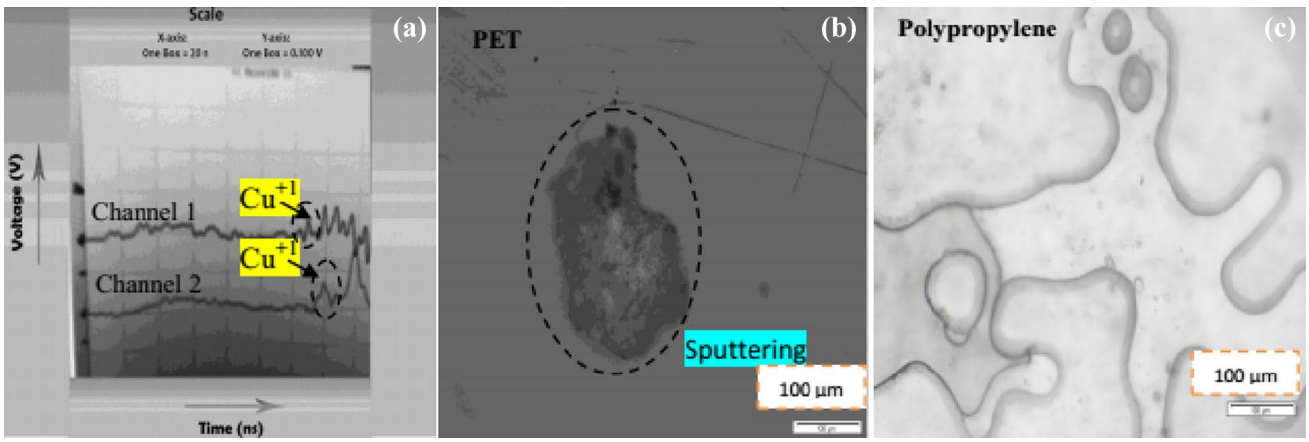

Fig. 12 **a** Faraday cup signal profile of Cu ions in air at an acceleration voltage of 14 kV and optical micrographs of ion irradiated, **b** PET, and **c** polypropylene (×200 magnifications)

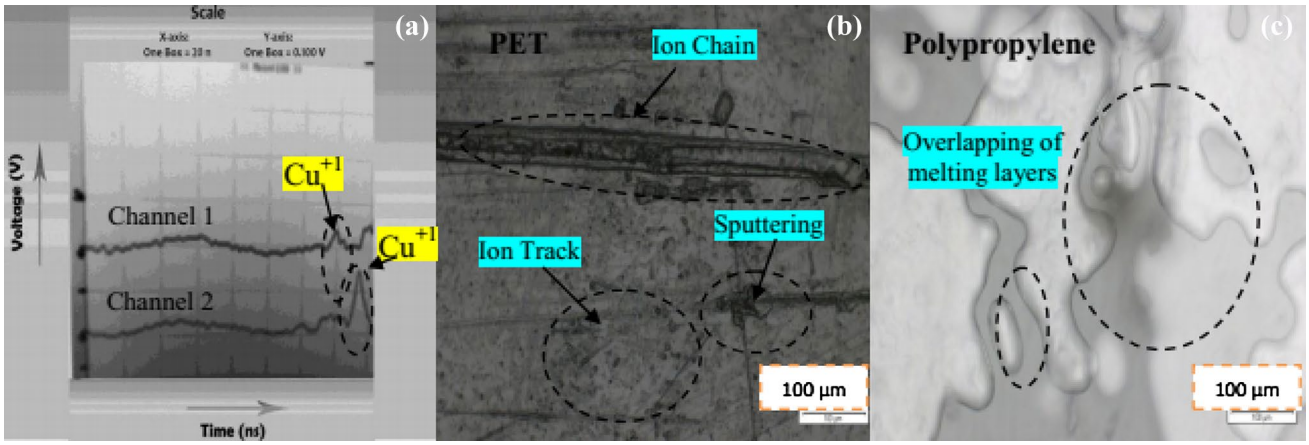

Fig. 13 **a** Faraday cup signal profile of Cu ions in air at an acceleration voltage of 16 kV and optical micrographs of ion irradiated, **b** PET, and **c** polypropylene (×200 magnification)

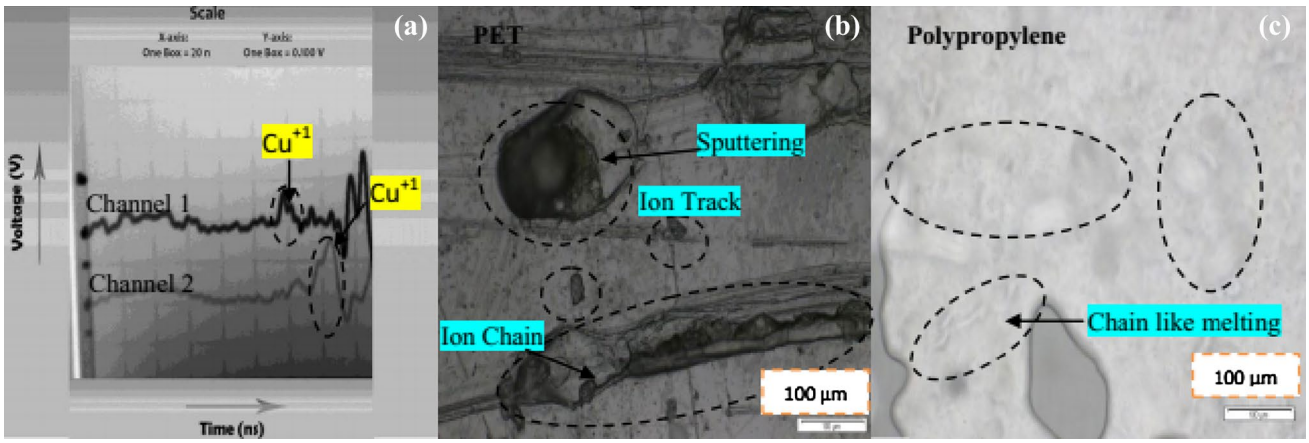

Fig. 14 **a** Faraday cup signal profile of Cu ions in air at an acceleration voltage of 18 kV and optical micrographs of ion irradiated, **b** PET, and **c** polypropylene (×200 magnification)

Table 1 Variations in conductivity concerning the average kinetic energy of the accelerated Cu^{1+} ions

Sr. no.	Applied voltage (kV)	Average kinetic energy of accelerated ions (keV)	PET conductivity ($\times 10^{-11}$ Mho-cm^{-1})	PP conductivity ($\times 10^{-11}$Mho-cm^{-1})
1.	0	490	1.378	6.26
2.	2	548	1.494	6.484
3.	4	569	1.52	6.658
4.	6	592	1.534	6.735
5.	8	614	1.601	7.026
6.	10	635	1.613	7.0469
7.	12	657	1.627	7.21
8.	14	680	1.78	8.024
9.	16	706	1.865	8.384
10.	18	730	2.065	8.49

charged as well as doubly charged Cu ions were detected, and at channel 2 a single burst of ion which contained Cu^{2+} and $Cu^{1+}$was detected. The peak of the doubly charged ions appears first, which is attributed to the fact that it has high velocity as well as kinetic energy compared to that of singly charged ions. The average kinetic energy of the accelerated ions is strongly dependent on the velocity of the ions. It has been observed that the singly charged Cu ions are in excessive amount for this laser intensity. It has been investigated that the doubly charged ions are, in general, emitted along the normal to the target material, whereas the singly charged ion emissions occur slightly off-axis but remain within the particular range. The initial peak of doubly charged ions Cu^{2+} has lower flux as compared to that of the second peak of singly charged ions Cu^{1+}; as a result, it gives the impression that the single charge ion emission is dominant in laser-generated copper plasma in our case.

Figure 5b, c represents the exposed samples of PET and polypropylene that were examined under the optical microscope. Both substrates (PET and polypropylene) were implanted via metallic Cu ions produced by exposing the target to 500 laser shots. The interaction of the energetic ions with polymeric materials leads to bond breaking, formation of free radicals and various phenomena that are induced by the complex secondary chemical processes along the trajectory of the ions. In polymers, the ionization and electronic excitation processes are known to lead to both chain scission and cross-linking. Ion implantation readily ruptures the carbon–hydrogen bond current in most polymeric materials and the mobile hydrogen atoms are able to escape. The irradiated part of the substrate is point out by dotted line circles. The ion beam-irradiated surface may have characteristics different from the pristine sample. Figure 5b, c shows the crater formation in the case of polyethylene terephthalate, and destruction, melting and track formation in the case of polypropylene. It was observed that damage was less in the case of untreated polyethylene terephthalate due to the effect of greater melting temperature (260 °C) as compared to polypropylene (130 °C). It is noted that the degree of surface modification is associated with the type of implanted ion and the energy of the ions.

Implantation of metallic Cu ions formed small craters at the surface of polyethylene terephthalate and produced chain-like melted structure in the case of polypropylene, which explains the destruction of previous bonds and the ions that have cross-linked to form new bonds as depicted in Fig. 6b, c. The manifestation of ion tracks confirms the modification in the surface morphology and the change in the chemical structure. In case of polymeric materials, ion implantation produces cross-linking and cross scission so that it will form protruding structure, such as hillocks instead of hole formation. It has been observed from Fig. 7b, c that the increase in the energy of ions increases the surface structure modification of the polymeric material. Note that by means of applied voltage of 4 kV, the kinetic energy of 569 keV produces chain-like structure at the surface of PET which is associated with the overlapping of the multi-bursts of ions at the same region in a specific manner. Due to energetic ion irradiation, destruction occurs in the case of polypropylene. The burst of ions damaged the structure of the substrate by breaking the bonds and further bursts of energetic ions rearranged the covalent bond and cross-linking occurred.

In Fig. 8, the optical micrograph of irradiated polyethylene terephthalate substrate shows that more energetic ions damaged the greater region of the surface and also more chains were observed. The diameter of the ion tracks increases in the case of polypropylene. Moreover, we have observed overlapped melted structures at the surface of polypropylene due to abrupt change in temperature. Since the ion-implanted polymer transformation is confined by a small track volume for every ion, the number of high-energy ions bombarding the polymer surface, or in other words, ion dose, is also a decisive parameter for material modifications. Figure 9a illustrates that the surface morphology becomes coarse and bumpy compared to that of ion-implanted substrates with ion energy.

It was found that the bumps are destroyed as the energy of the incident ions increases and the surface becomes foam-like smooth as shown in Fig. 10c. During the high-energy metal ion implantation, the surface sputtering effect was observed as given in Fig. 10b in the case of polyethylene terephthalate. It has been observed that by increasing the energy of metallic ions, more region is damaged due to ion sputtering and also ion tracks are formed as shown in Fig. 11b. The structure of the polypropylene is damaged up to a certain region due to melting and re-solidification of substrate that is strongly affected by the bursts of energetic ions as given in Fig. 11c.

The optical micrograph of one part of the substrate PET shows that the high-energy Cu ions cause the effect of sputtering and the melted zone is also observed at the edges of the ion track formation as shown in Fig. 12b. Figure 12c shows the small bubble formation and overlapped melted layers due to high-energy ion irradiation. The succeeding overlap of many ion tracks in the same region is required to acquire a complete change of the bonding scheme at high-energy and/or high-fluence irradiated material as shown in Fig. 13b. The surface morphology of the polypropylene reveals that the surface becomes smoother due to multi-layer overlapping of melted material as given in Fig. 13c. The formation of tracks of energetic ions can be used to modify the physical and chemical properties of polymers. The intensity of the modification could also be controlled by varying

the implanted dose. High-energy ion implantation of polymeric materials results in degradation of the organic host due to significant modification of chemical bonds as shown in Fig. 14b, c. There are two possible competing processes, i.e., one is the scission of molecular polymer chain resulting in fractionating and the second is free radical formation (branching) leading to cross-linking and bond conjugation. The effectiveness of branching is intimately related to the type of polymer.

From numerous studies that have been made of the effects of using different ion beams, it has been possible to deduce that the energy deposited in ionizing of electron-exciting processes is more effective for hardening than atomic collision, or elastic processes. The latter tends to induce chain scission. With regard to such simple geometric factor as the track radius, it is easy to understand that there is threshold fluence, at which the substrate surface appears to be totally filled with ion tracks. The separated ion track damaged volumes start overlapping, and further irradiation thus carries out into the already modified material. In this way, one can differentiate two implantation regimes: (a) a single ion track regime when the tracks are secluded (isolated) from each other and (b) a track overlapping regime.

3.2 Electrical conductivity of ion-irradiated PET and polypropylene

Figure 15 presents the variations in conductivity concerning the average kinetic energy of the accelerated Cu^{1+} ions and the related values are enlisted in Table 1. It is clear from Fig. 15 and Table 1 that the electrical conductivity of PET is an increasing function of the ion implantation energy. Such an increase in the electrical conductivity can be explained on the basis of the reality that high-energy ion implantation in polymeric materials leads to the formation of free radicals, dangling bonds and liberation of low molecular weight volatile species such as hydrogen, ensuing in the creation of cross-linked carbonaceous clusters on the implanted surface of the polymer and offer a continuous path for the charge transfer within the insulating polymer chains. The formation of such a cross-linked arrangement responsible for the enhanced electrical conductivity after ion implantation can be explained in terms of the linear energy transfer by the implanted ions in the subsequent manner. When energetic ions shower on the surface of the polymer, they lose energy, liberate hydrogen and form a carbon-enriched structure. This kind of carbon-enriched bunch is more conductive than the pristine polymer region. If ion dose or energy is increased, many of these clusters (bunches) will initiate to contact each other and in conclusion overlap to form a continuous carbon-rich conductive surface. It contributes to the measurable electrical conductivity of polymers.

It is clear from Fig. 15 that the electrical conductivity of the pristine sample is low as compared to the metal ion-implanted PET. Figure 16 confirms the deviation in electrical conductivity regarding the average kinetic energy of the accelerated Cu^{1+} ions and the corresponding values are enlisted in Table 1. It has been observed that the conductivity of PET is an increasing function of the ion implantation energy. It is unambiguous from Fig. 16 that there is almost linear variation in electrical conductivity of polypropylene with respect to energy. It was also found that the conductivity values of ion-irradiated polypropylene rise significantly compared to that of ion-implanted PET. This can be recommended due to

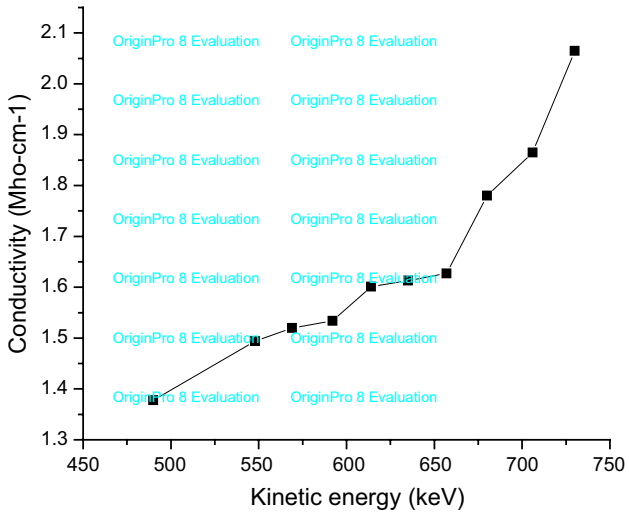

Fig. 15 Plot of conductivity vs energy of Cu ion-implanted PET

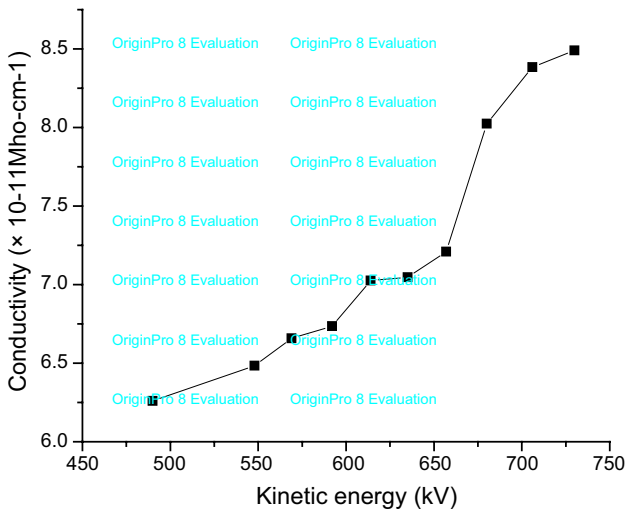

Fig. 16 Plot of electrical conductivity vs average kinetic energy of accelerated Cu ion-implanted polypropylene

the effect of the large penetration depth of metallic ions inside polypropylene as compared to that of PET. Additionally, the experiential changes in the electrical conductivity of ion-implanted PET and polypropylene may be due to the integrated structural changes as a result of Cu ion implantation.

4 Conclusion

In this paper, home-made cost-effective, compact and versatile tabletop laser-driven accelerator as ion source, employing an external positive electric field (+HV, DC) for ion acceleration, was set up, characterized and tested for implantation. It was observed that the average kinetic energy of the Cu ions is a function of the externally applied acceleration voltage. Increased energy of the laser-generated ions is due to the acceleration potential, and the maximum energy measured was 730 keV at an acceleration voltage of +18 kV. The experimental analysis of optical micrographs of the implanted PET and polypropylene confirmed the increase in the damage, such as ion track, bubble and ion chain formation, sputtering and melting, produced by metallic (Cu) ions with increasing energy. The increased electrical conductivity of high-energy Cu ion-implanted PET and polypropylene was possibly due to the formation of three-dimensional carbonaceous network consisting of the disordered bonds emerging in the irradiated layer of both substrates. An increase in the value of electrical conductivity was found due to the effect of increasing energy of metallic ions. The results of the present study point out that the ion implantation through this accelerator has the potential to become an important tool for modification of solids, to improve the material properties.

References

1. Y. Wu, T. Zhang, Y. Zhang, H. Zhang, X. Zhang, G. Zhou, Nucl. Instrum. Methods Phys. Res. **B 173**, 292–298 (2001)
2. Y. Lee, S. Han, H. Lim, Y. Kim, H. Kim, Anal. Bioanal. Chem. **373**, 595–600 (2002)
3. G.B. Hadjichristov, V.K. Gueorguiev, T.E. Ivanov, Y.G. Marinov, V.G. Ivanov, E. Fau, J. Phys: Conf. Ser. **207**, 1–4 (2010)
4. V.Y. Fominakii, A.G. Gnedovets, A.V. Khoromanskaya, Russ. Res. **28**, 1091–1097 (2008)
5. Vladimir N. Popok, Rev. Adv. Mater. Sci. **30**, 1–26 (2012)
6. L. Torrisi, G. Ciavola, S. Gammino, L. Andò, A. Barnà, Rev. Sci. Instr. **71**(11), 4330–4334 (2000)
7. M.B. Tahir, M. Rafique, M.S. Rafique, T. Iqbal, G. Nabi, Indian J. Pure Appl. Phys. **55**, 145–154 (2017)
8. F. Belloni, Ion implantation via a Laser ion source, Ph. D thesis, 2006
9. J. Wolowski, P. Parys, E. Woryna, J. Krása, L. Láska, K. Rohlena, S. Gammino, G. Ciavola, L. Torrisi, F.P. Boody, R. Höpfl, H. Hora, H. Haseroth, Opt. Appl. **30**(1), 69–82 (2000)
10. M.C. Salvadori, M. Cattani, F.S. Teixeira, I.G. Brown, Appl. Phys. Lett. **93**, 073102 (2008)
11. G.M. Petrov, J. Davis, Appl. Phys. B **96**, 773 (2009)
12. L. Torrisi, S. Gammino, L. Andò, Radiat. Eff. Defects Solids **157**, 333–346 (2002)
13. K. Rohlena, L. Láska, K. Jungwirth, J. Krása, E. Krouský, M. Mašek, M. Pfeifer, J. Badziak, P. Parys, T. Pisarczyk, J. Woowski, S. Gammino, L. Torrisi, J. Phys. IV **133**, 1111–1116 (2006)
14. A. Lorusso, V. Nassisi, L. Velardi, A.C. Rainò, L. Torrisi, D. Margarone, Radiat. Eff. Defects Solids **163**, 447–451 (2008)
15. G.D. Girolamo, M. Massaro, E. Piscopiello, L. Tapfer, Nucl. Instrum. Methods Phys. Res. **B 268**, 2878–2882 (2010)
16. A. Sharma, K.D. Verma, M. Varshney, D. Singh, M. Singh, K. Asokan, R. Kumar, Plasma Sci. Plasma Technol. **165**, 930–937 (2010)
17. L. Yeonhee, H. Seunghee, L. Hyuneui, J. Hyesun, C. Junghee, K. Youngwoo, J. Appl. Polym. Sci. **60**, 2227–2238 (1996)
18. H. Seunghee, L. Yeonhee, H. Kim, G.-H. Kim, J. Lee, J.-H. Yoon, G. Kim, Surf. Coat. Technol. **93**, 261–264 (1997)
19. E.C. Rangel, N.C. Dacruz, M.H. Tabacniks, C.M. Lepienski, Nucl. Instrum. Methods Phys. Res. **B 175–177**, 594–598 (2001)
20. G.M. Chan, T.M. Ko, H. Hiraoka, Surf. Sci. Rep. **24**, 1–54 (1996)
21. L. Torrisi, A.M. Mezzasalma, S. Gammino, J. Badziak, P. Parys, J. Wolowski, L. Laska, Franco. Appl. Surf. Sci. **252**, 8533–8538 (2006)
22. G.R. Rao, K. Monar, E.H. Lee, J.R. Treglio, Surf. Coat. Technol. **64**, 69–74 (1994)
23. W. Yuguang, Z. Tonghe, L. Andong, Z. Xu, Z. Gu, Vacuum **69**, 461–466 (2003)
24. E.C. Rangel, N.C. da Cruz, M.A.B. de Moraes, C.M. Lepienski, Surf. Coat. Technol. **127**, 93–98 (2002)
25. P.K. Goyal, Gupta R. KumarV, S. Kumar, P. Kumar, D. Kanjilal, AIP Conf. Proc. **1393**, 147–148 (2011)
26. R.S. Kohlman, A. Zibold, D.B. Tanner, G.G. Ihas, T. Ishiguro, Y.G. Min, A.G. MacDiarmid, A.J. Epstein, Phys. Rev. Lett. **78**, 3915–3918 (1997)
27. D. Sinha, Adv. Appl. Sci. Res. **3**(3), 1365–1371 (2012)
28. D. Fink, P.S. Alegaonkar, A.V. Petrov, M. Wilhelm, P. Szimkowiak, M. Behar, D. Sinha, W.R. Fahrner, K. Hoppe, L.T. Chadderton, Nucl. Instrum. Methods Phys. Res. **B 236**, 11–20 (2005)
29. Huiyun Feng, Yu. Zengliang, Paul K. Chu, Mater. Sci. Eng. R **54**, 49–120 (2006)
30. N. Singh, A. Sharma, D.K. Avasthi, Nucl. Instrum. Methods Phys. Res. **B 206**, 1120–1123 (2003)
31. R. Gupta, V. Kumar, P.K. Goyal, S. Kumar, S.L. Goyal, Adv Appl. Sci. Res. **3**(5), 2766–2773 (2012)
32. S. Bagchi, P. Prem Kiran, M.K. Bhuyan, S. Bose, P. Ayyub, Appl. Phys. B **88**, 167 (2007)
33. L. Torrisi, S. Gammino, L. Andò, L. Laska, J. Krasa, J. Appl. Phys. **91**(7), 4685–4692 (2002)
34. S. Gammino, L. Torrisi, G. Ciavola, L. Andò, J. Wolowski, L. Laska, Nucl. Instrum. Methods **209**, 345–350 (2003)
35. K. Rohlena, L. Láska, K. Jungwirth, J. Krása, E. Krouský, M. Mašek, M. Pfeifer, J. Ullschmied, J. Badziak, P. Parys, J. Wołowski, S. Gammino, L. Torrisi, F.P. Boody, Plasma Phys Contr. Fusion **47**, B503–B512 (2005)
36. J. Wolowski, J. Badziak, F.P. Boody, A. Czarnecka, S. Gammino, S. Jablonski, J. Krasa, L. Laska, P. Parys, K. Rohlena, M. Rosinski, L. Ryc, L. Torrisi, J. Ullschmied, Plasma Phys. Control. Fusion **48**, B475–B482 (2006)
37. L. Laska, J. Badziak, F.P. Boody, S. Gammino, K. Jungwirth, J. Krasa, E. Krousky, P. Parys, M. Pfeifer, K. Rohlena, L. Ryc, J.

Skala, L. Torrisi, J. Ullschmied, J. Wolowski, Laser Part. Beams **5**(2), 199–205 (2007)
38. L. Láska, J. Krása, M. Pfeifer, K. Rohlena, S. Gammino, L. Torrisi, G. Ciavola, L. Andò, Rev. Sci. Instr. **75**(5), 1575–1578 (2004)
39. R. Ahmed, M.S. Rafique, M.B. Tahir, H. Malik, Laser Part. Beams **32**(2), 261–270 (2014)
40. L. Torrisi et al., Nukleonika **57**, 323–332 (2012)
41. V. Popok, Rev. Adv. Mater. Sci. **30**(1), 1–26 (2012)
42. M. Masuda, N. Tanaka, K. Hane et al., Appl. Phys. B **119**, 421 (2015)